Sensitivity of the Ocean's Climate to Diapycnal Diffusivity in an EMIC. Part II: Global Warming Scenario

FABIO DALAN, PETER H. STONE, AND ANDREI P. SOKOLOV

Joint Program on the Science and the Policy of Climate Change, Massachusetts Institute of Technology, Cambridge, Massachusetts

(Manuscript received 9 April 2004, in final form 15 December 2004)

ABSTRACT

The sensitivity of the ocean's climate to the diapycnal diffusivity in the ocean is studied for a global warming scenario in which CO_2 increases by 1% yr^{-1} for 75 yr. The thermohaline circulation slows down for about 100 yr and recovers afterward, for any value of the diapycnal diffusivity. The rates of slowdown and of recovery, as well as the percentage recovery of the circulation at the end of 1000-yr integrations, are variable, but a direct relation with the diapycnal diffusivity cannot be found. At year 70 (when CO_2 has doubled) an increase of the diapycnal diffusivity from 0.1 to 1.0 $cm^2\ s^{-1}$ leads to a decrease in surface air temperature of about 0.4 K and an increase in sea level rise of about 4 cm. The steric height gradient is divided into thermal component and haline component. It appears that, in the first 60 yr of simulated global warming, temperature variations dominate the salinity ones in weakly diffusive models, whereas the opposite occurs in strongly diffusive models.

The analysis of the vertical heat balance reveals that deep-ocean heat uptake is due to reduced upward isopycnal diffusive flux and parameterized-eddy advective flux. Surface warming, induced by enhanced CO_2 in the atmosphere, leads to a reduction of the isopycnal slope, which translates into a reduction of the above fluxes. The amount of reduction is directly related to the magnitude of the isopycnal diffusive flux and parameterized-eddy advective flux at equilibrium. These latter fluxes depend on the thickness of the thermocline at equilibrium and hence on the diapycnal diffusion. Thus, the increase of deep-ocean heat uptake with diapycnal diffusivity is an indirect effect that the latter parameter has on the isopycnal diffusion and parameterized-eddy advection.

1. Introduction

Climate models are very sensitive to the diapycnal diffusivity, both for the equilibrium climate state (Bryan 1987; Marotzke 1997; Zhang et al. 1999; Park and Bryan 2000) and in transient experiments, triggering strong nonlinear behavior (Ganopolsky et al. 2001; Manabe and Stouffer 1999). Yet, the global averaged value of the diapycnal diffusivity is uncertain. Measurements of the diapycnal diffusivity are localized in space and time (Polzin et al. 1997; Ledwell et al. 2000) while calculations of the global averaged diapycnal diffusivity vary as much as a factor 5 (Munk and Wunsch 1998; Huang 1999). In Part I of this study we analyzed the sensitivity of the current climate to the diapycnal diffusivity (Dalan et al. 2005). In this paper we illustrate the influence of the diapycnal diffusivity on the transient behavior of the thermohaline circulation (THC) and on the rate of change of heat content, sea surface temperature, and sea level rise.

The THC appears to be driven by the steric height gradient between North and South Atlantic (Hughes and Weaver 1994). By changing the relative strength of the processes transporting heat and salt in the ocean, positive feedbacks may strengthen, triggering strong nonlinear behavior in the THC evolution. By changing the rate of CO_2 increase in the atmosphere, Stocker and Schmittner (1997) observed a slowdown and recovery of the THC or a complete collapse of the THC for slow and fast rates respectively. The same pattern was observed by Ganopolsky et al. (2001), varying both vertical diffusivity and hydrological sensitivity in a 2D multibasin ocean model coupled with a 2D statistical-dynamical model. For low vertical diffusivity and high hydrological sensitivity, the THC shuts down in a simulation with 1% CO_2 rate of increase for 140 yr and constant afterward (stabilization at $4 \times CO_2$). For all

Corresponding author address: Fabio Dalan, Via Cavour 44/e, 35030 Rubano (PD), Italy.
E-mail: fabio.dalan@alum.mit.edu

the other combinations of the two parameters the strength of the THC decreases for about 150 yr and then partially recovers. This study will extend Ganopolsky et al. (2001) results by using a 3D ocean model coupled with a 2D atmosphere and varying only the diapycnal diffusivity. Furthermore, the change in steric height gradient is divided into thermal component and haline component and the relative magnitude of the components is analyzed with respect to changes in the diapycnal diffusivity.

In the last Intergovernmental Panel on Climate Change (IPCC) report (Houghton et al. 2001), the results from model projections of leading research groups are presented. Among other quantities, models are commonly compared in terms of surface air temperature (SAT) change and sea level rise (SLR). All models simulate an increase in surface air temperature and sea level, as a consequence of an increase of CO_2 in the atmosphere, but the magnitude of the increase varies as much as a factor of three. Both SAT and SLR due to thermal expansion depend on the rate of deep-ocean heat uptake. The rate of increase of SAT depends on the effective heat capacity of the Earth system. Because of the large heat capacity of water compared to air and land, the heat capacity of the combined atmosphere–land–ocean system depends on the portion of ocean that will be affected by global warming, therefore on the rate of ocean heat uptake. The sea level rises mainly because the volume of the water increases with temperature; therefore, it also depends on the rate at which the ocean takes up heat.

The rate of ocean heat uptake is not well constrained by observations of the temperature record of the past 50 yr (Forest et al. 2002) and varies greatly among models (Sokolov et al. 2003). Hence, detailed studies on the vertical heat balance in the ocean are needed in order to understand which processes and parameters control the rate of ocean heat uptake in numerical models. Two studies of this kind are presented by Gregory (2000) and Huang et al. (2003c). In the first study advective fluxes (Eulerian and parameterized-eddy velocity advection) and diffusive fluxes (isopycnal and diapycnal) are combined together, when analyzing the global ocean balance, and the balance for different latitude bands and basins is limited to a single depth level (160 m). We will hereafter refer to the parameterized-eddy advective flux as the GM flux from the commonly used Gent–McWilliams parameterization (Gent and McWilliams 1990). Huang et al. (2003a,b,c) combine together the isopycnal diffusive flux and the GM flux. Their adjoint sensitivity studies show that the heat content of the ocean and its change in transient climate scenarios is dependent on these combined fluxes (Huang et al. 2003a,b). However, varying both the isopycnal and thickness diffusivities simultaneously does not change appreciably the rate of ocean heat uptake (Huang et al. 2003c). In this paper, the vertical heat flux of the ocean is divided into all its components and for every depth level. Moreover the sensitivity of the rate of deep-ocean heat uptake to diapycnal diffusivity is presented for a standard global warming scenario. For the sensitivity of the vertical heat balance at equilibrium refer to Dalan et al. (2005).

Uncertainty in the heat uptake is a major source of uncertainty in global warming projections (Webster el al. 2003). Sokolov et al. (2003) found that the difference in the heat uptake simulated by coupled atmosphere–ocean GCMs (AOGCMs) could be described by differences in the rate at which heat anomalies are effectively diffused into the ocean. Using the Sokolov et al. (2003) model to fit the trend of the Massachusetts Institute of Technology (MIT) earth model of intermediate complexity (EMIC), we will relate the diapycnal diffusivity to the effective vertical diffusivity of Sokolov et al. (2003).

The paper is organized as follows: in section 2 we briefly describe the numerical model; in section 3 we analyze the transient behavior of the THC circulation for simulations with different diapycnal diffusivity; section 4 contains the sensitivity of the ocean heat uptake, SAT and SLR to the diapycnal diffusivity; finally, section 5 contains a review of the results.

2. MIT earth model of intermediate complexity

More details of the model can be found in Kamenkovich et al. (2002).

a. Atmospheric component

The two-dimensional zonally averaged statistical-dynamical atmospheric model was developed by Sokolov and Stone (1998) on the basis of the Goddard Institute for Space Studies (GISS) GCM (Hansen et al. 1983). The model solves the zonally averaged primitive equations in latitude-pressure coordinates. The grid of the model consists of 24 points in the meridional direction, corresponding to a resolution of 7.826°, and nine layers in the vertical. Moreover, the model includes the parameterization of heat, moisture and momentum transports by large-scale eddies (Stone and Yao 1990) and has a complete moisture and momentum cycle.

Most of the physics and parameterizations of the atmospheric model derive from the GISS GCM. The 2D model, as well as the GISS GCM, allows four different types of surfaces in the same grid cell, namely, open

ocean, sea ice, land, and land ice. The surface characteristics, as well as turbulent and radiative fluxes, are calculated separately for each kind of surface, while the atmosphere above is assumed to be well-mixed zonally. The atmospheric model uses a realistic land/ocean ratio at each latitude band. More detailed description of this part of the model can be found in Sokolov and Stone (1998) and Prinn et al. (1999).

The dependence of zonal-mean surface fluxes of heat and momentum on surface warming simulated by this model coupled to a 2D ocean model is similar to that shown by more sophisticated atmospheric GCMs (Sokolov and Stone 1998; Prinn et al. 1999). Moreover, vertical and latitudinal structure of the 2D model response is also consistent with the results of different GCMs. However, such a model cannot represent feedbacks associated with changes in the ocean circulation. To take into account possible interactions between atmosphere and ocean circulation, the 2D ocean model is replaced, in this study, by a 3D ocean GCM with simplified geometry.

b. Ocean component

The ocean component of the coupled model is the modular ocean model (MOM2; Pacanowski 1996) with idealized geometry. It consists of two rectangular "pool" basins connected by a Drake Passage that extends from 64° to 52°S. The Indo-Pacific (hereinafter Pacific) pool extends from 48°S to 60°N and is 120° wide while the Atlantic pool extends from 48°S to 72°N and is 60° wide. The meridional resolution is 4° and the zonal resolution varies from 1° near the north–south boundaries to 3.75° in the interior of the ocean. In the vertical, the model has 15 layers of increasing thickness from 53 m at the surface to 547 m at depth. The bottom of the ocean is flat and 4500 m deep everywhere except in the Drake Passage where there is a sill 2900 m deep.

No-slip boundary conditions are applied to the lateral walls and free-slip boundary conditions at the bottom of the ocean, except in the Antarctic Circumpolar Current (ACC) where bottom drag is applied so as to obtain a more realistic speed for the ACC. Boundary conditions for tracers are insulating at lateral walls and bottom of the ocean. A mixed layer model adopted from the GISS GCM replaces the ocean GCM southward of 64°S and northward of 72°N. The depth of the mixed layer is prescribed from observations as a function of latitude and time. In climate change simulations, heat penetrating into the ocean below the mixed layers is parameterized by diffusion of the deviation of the mixed layer temperature from its present-day climate values. Moreover, any changes in the runoff are evenly distributed throughout the ocean at any given time.

The Gent–McWilliams parameterization scheme is used to account for the small-scale eddy induced transport (Gent and McWilliams 1990). Mixing caused by small-scale processes occurs along and across isopycnals (Redi 1982). No background horizontal diffusivity is used. The surface boundary conditions used to spin up the ocean model are taken from Jiang et al. (1999) who constructed the datasets using a variety of sources.

c. Coupling, spinup, and experimental setup

Coupling takes place twice a day. The atmospheric model calculates 12-h mean values of the wind stress, heat, and freshwater fluxes over the open ocean and their derivatives with respect to the SST. These quantities are then linearly interpolated to the oceanic grid. The derivatives of the surface fluxes with respect to the SST are multiplied by the deviation of the SST from its zonal mean. This term is then added to the atmospheric surface fluxes and passed to the ocean model. This procedure allows one to account for the zonal variations of the surface fluxes. The coupling procedure uses flux adjustments. The adjustments are given by the difference between the surface fluxes diagnosed after the spinup of the ocean-only model and the fluxes generated in the spinup of the atmospheric model alone forced by observed SST and sea ice distribution. The ocean is integrated for 12 h and provides to the atmosphere the zonal mean SST. Asynchronous integration is used (Bryan 1984), with 12 h time step for the tracer equations and 1 h time step for the momentum equations. For more details on the coupling procedure see Dalan et al. (2005) and Kamenkovich et al. (2002).

After separate spinup of the atmospheric and oceanic components the model has been coupled and spun up for 1000 yr for each value of the diapycnal diffusivity: 0.1, 0.2, 0.5, and 1.0 $cm^2\ s^{-1}$. The model was considered to be at equilibrium when the global average heat flux entering the ocean fluctuates around the zero value. In the global warming experiments, the CO_2 in the atmosphere increases by 1% yr^{-1} for 75 yr and then it is kept constant for 925 yr. Control runs are also performed starting at the end of the coupled spinup, with constant CO_2 concentration for 1000 yr. As a measure of the transient climate change at the time of CO_2 doubling we take the difference between the mean climate in the global warming experiments and the control climate averaged over years 66–75.

3. Behavior of the thermohaline circulation

In our model the thermohaline circulation slows down as a consequence of enhanced CO_2 in the atmo-

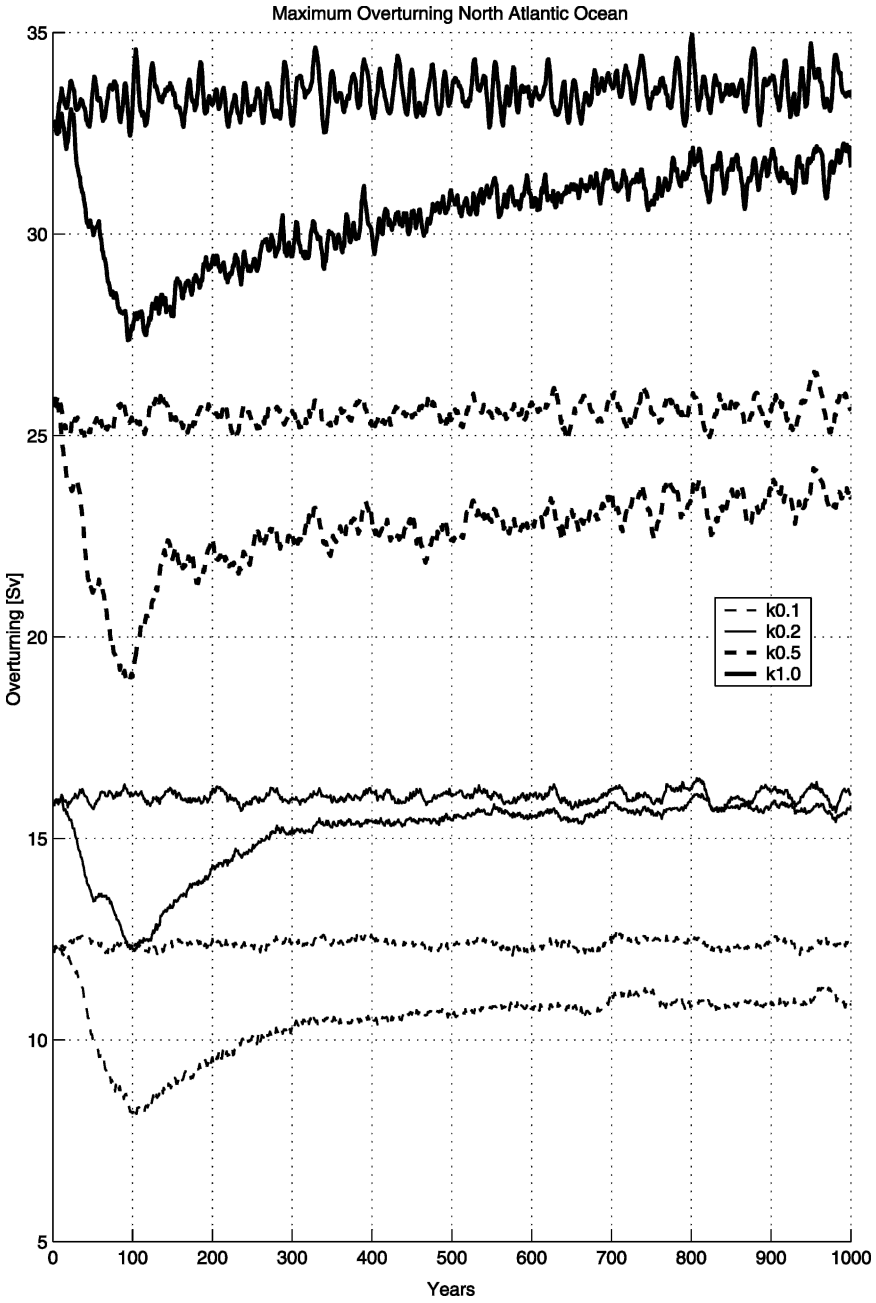

FIG. 1. Maximum meridional streamfunction in the North Atlantic Ocean. For each value of the diapycnal diffusivity, both control experiment and global warming overturning strength is displayed. The control overturning strength of the THC fluctuates around a mean value that depends on the diapycnal diffusivity. In global warming experiments the THC strength diminishes for about 100 yr and then partially or fully recovers its original value. Diffusivity 0.1 $cm^2\ s^{-1}$, thin dashed line; 0.2 $cm^2\ s^{-1}$, thin solid line; 0.5 $cm^2\ s^{-1}$, thick dashed line; and 1.0 $cm^2\ s^{-1}$, thick solid line.

sphere (Fig. 1), as it does in most CMIP2 (Coupled Model Intercomparison Project) models. For each global warming simulation with different diapycnal diffusivity, the strength of circulation in the Atlantic Ocean decreases for 100 yr, 25 yr after the stabilization of the CO_2, and it recovers afterward. Hence, the behavior of the system to changes in diapycnal diffusivity is self-similar. Ganopolsky el al. (2001) found strong

nonlinear behavior of the THC varying both vertical diffusivity and hydrological sensitivity.[1] For small vertical diffusivity and large hydrological sensitivity the THC shuts down for a 1% CO_2 increase for 140 yr, while for all other combinations of the two parameters the THC slows down and then partially recovers. Our model is extremely stable to freshwater perturbations, as inferred from the hysteresis curves presented in Dalan et al. (2005). Moreover, we do not register major changes in freshwater flux in the North Atlantic as a consequence of global warming (Kamenkovich et al. 2003).

The rate and the amount of recovery vary for each experiment in an unpredictable way. For example, the simulation with diffusivity 0.5 $cm^2\ s^{-1}$ presents the fastest recovery although it is with the diffusivity 0.2 $cm^2\ s^{-1}$ that the circulation first fully recovers its strength (Fig. 1). Moreover, the natural variability of the THC in the control run increases with the diapycnal diffusivity, its value going from 0.2 Sv for the 0.1 $cm^2\ s^{-1}$ diffusivity to 1 Sv for the 1.0 $cm^2\ s^{-1}$ diffusivity. The behavior of the circulation depicted in Fig. 1 raises the question of the predictability of the THC in global warming experiments (Knutti and Stocker 2002). Regardless of the path followed in the recovery, the new equilibrium achieved after the CO_2 stabilization, presents a shallower overturning circulation (not shown), as noted by Huang et al. (2003c). As a consequence of the THC slowdown, the bottom of the ocean fills up with cold water, which represents an obstacle for the water sinking in the North Atlantic when the circulation recovers. Little changes are registered in the rate of Antarctic Bottom Water (AABW) formation. This may be due to our model configuration as extending the Drake Passage all the way to Antarctica inhibits the AABW formation in ocean GCMs with idealized topography (Hughes and Weaver 1994).

The steric height is the integrated pressure from the surface to a reference depth; hence, it is proportional to the quantity

$$P = \int_{z^*}^{0} \int_{z}^{0} \frac{\rho}{\rho_o}\, dz'\, dz,$$

where ρ is the in situ density, ρ_0 is a reference density and z^* is a reference depth, in our case 3000 m. The THC strength at equilibrium is correlated to the steric height difference between the North and South Atlantic (Hughes and Weaver 1994; Thorpe et al. 2001). In the idealized geometry of the MIT EMIC, the steric height difference is not sensitive to the choice of the south Atlantic latitude, as long as the latter is located northward of the Drake Passage, while the North Atlantic latitude needs to be north of 60°N. The THC strength at equilibrium is best correlated to the steric height difference in the Atlantic Ocean when the latter is calculated between 30°S and 66°–70°N. Since the THC circulation is stronger for increasing diapycnal diffusivity, the gulf stream extends to higher latitudes for models with 0.5 and 1.0 $cm^2\ s^{-1}$ diapycnal diffusivity. Hence, for a fair comparison among simulations with different diapycnal diffusivity, the steric height is calculated between 30°S and 66°N for diffusivities 0.1 and 0.2 $cm^2\ s^{-1}$ and between 30°S and 70°N for diffusivities 0.5 and 1.0 $cm^2\ s^{-1}$.

Both the percentage reduction of the THC strength and steric height gradient decrease with increasing overturning (Fig. 2). However, the steric height gradient change does not correlate with the percentage recovery at the end of the integration. This indicates that the longitudinal variations of the steric height may be relevant to explain the transient behavior of the THC.

Since the steric height depends on the density of the water column, we want to quantify the relative importance of the temperature and salinity profile in determining the steric height gradient. Using the temperature field from the transient run and the salinity field from the control run, we can calculate the temperature contribution to the steric height gradient. The salinity contribution is computed with the same technique. The result is depicted in Fig. 3. For all simulations, the time series of the temperature and salinity contribution to the steric height gradient anomaly have a common trend, summarized as follows: at first, both temperature and salinity contributes to the decrease of the steric height gradient, while, after a certain time, temperature and salinity have opposite contributions to the steric height gradient (Fig. 3). The time at which the rate of change of the salinity contribution becomes positive is roughly 140 yr for the smallest diffusivities (0.1 and 0.2 $cm^2\ s^{-1}$) and 70 yr for the largest diffusivities (0.5 and 1.0 $cm^2\ s^{-1}$). Therefore we can identify two types of systems: a slow responding system for small diffusivities and a fast responding system for large diffusivities.

An important characteristic of the response of the system is the relative role of temperature and salinity in determining the steric height gradient in the first 75 yr of the transient runs. For slow responding systems, the temperature effect is always the dominant term (Figs. 3a,b). For fast responding systems, in the first decades of integration, the salinity anomalies have greater importance (Figs. 3c,d) than the temperature anomalies in determining the steric height gradient. At the time of

[1] The hydrological sensitivity allows one to regulate the amount of freshwater flux into the North Atlantic.

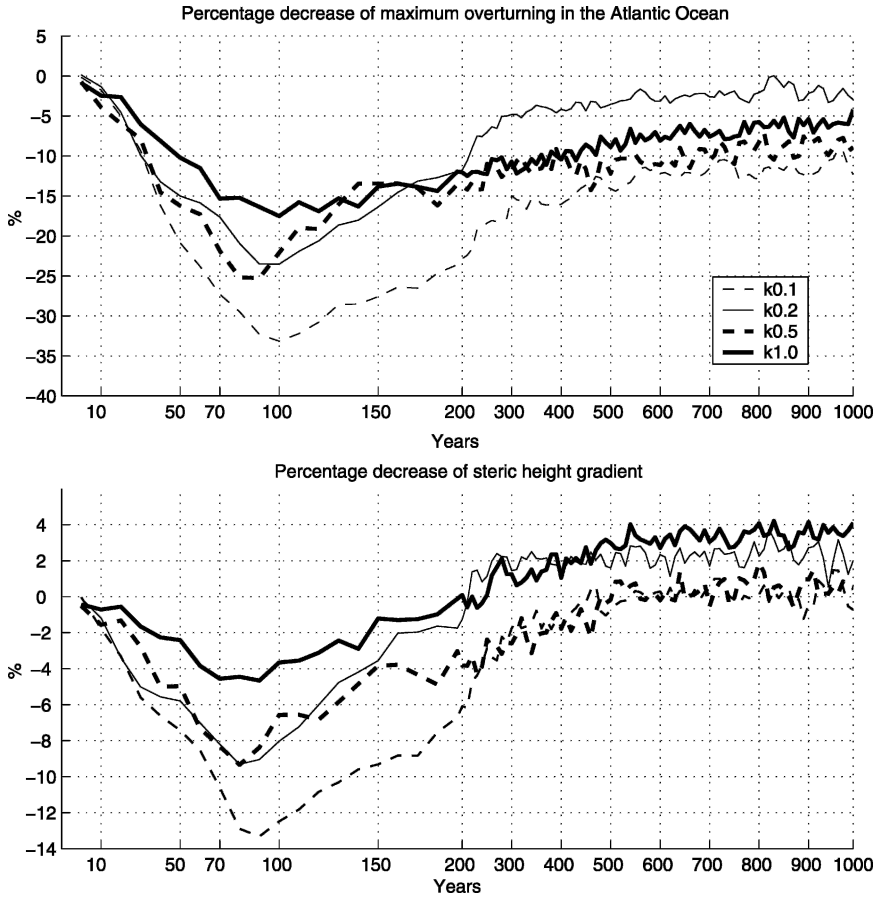

FIG. 2. Percentage reduction of (top) maximum meridional streamfunction and (bottom) steric height gradient in the Atlantic Ocean for different values of the diapycnal diffusivity: diffusivity 0.1 $cm^2\,s^{-1}$, thin dashed line; 0.2 $cm^2\,s^{-1}$, thin solid line; 0.5 $cm^2\,s^{-1}$, thick dashed line; and 1.0 $cm^2\,s^{-1}$, thick solid line. Note the stretching of the horizontal axis.

doubling of CO_2 however, the changes in the temperature distribution in the ocean are driving the steric height gradient for all the global warming simulations.

Thorpe et al. (2001) carried out a detailed analysis of the changes in steric height gradient. The authors concluded that, in the first 70 yr of global warming, at the surface fluxes of heat and freshwater tend to slowdown the THC, while the changes in the meridional heat and salt transport help the THC recovery. An examination of our results suggests that the salinity fluxes in the deep ocean are dominated by advection, both in the equilibrium and transient experiments. For the temperature contribution the situation is more complicated. Changes in the GM advection and isopycnal diffusion tend to warm the North Atlantic, as we will see in the next section. Moreover, the reduction of the THC implies a substantial reduction of the heat transport into high latitudes. This leads to a relative cooling of the North Atlantic and warming of the tropical Atlantic. Hence, changes in both GM advection and isopycnal diffusion decrease the steric height gradient while the decrease in meridional heat transport tends to increase it. Additionally, the density contribution of the heat flux at the surface in the North Atlantic in our model is about 7 times larger than the freshwater flux as shown by Kamenkovich et al. (2003, their Figs. 2a and 3).

The climate is a potentially chaotic system, therefore the realizations portrayed in Fig. 3 may depend on the initial condition. To further investigate this aspect, we perform another global warming experiment with diapycnal diffusivity 0.5 $cm^2\,s^{-1}$ starting from year 10 of the control run. Starting from a different initial condition slightly changes the relative importance of temperature and salinity in the first 70 yr of integration (not shown). In particular, in one case the salt component of the steric height anomaly is larger than the temperature component for about 65 yr of global warming; in the

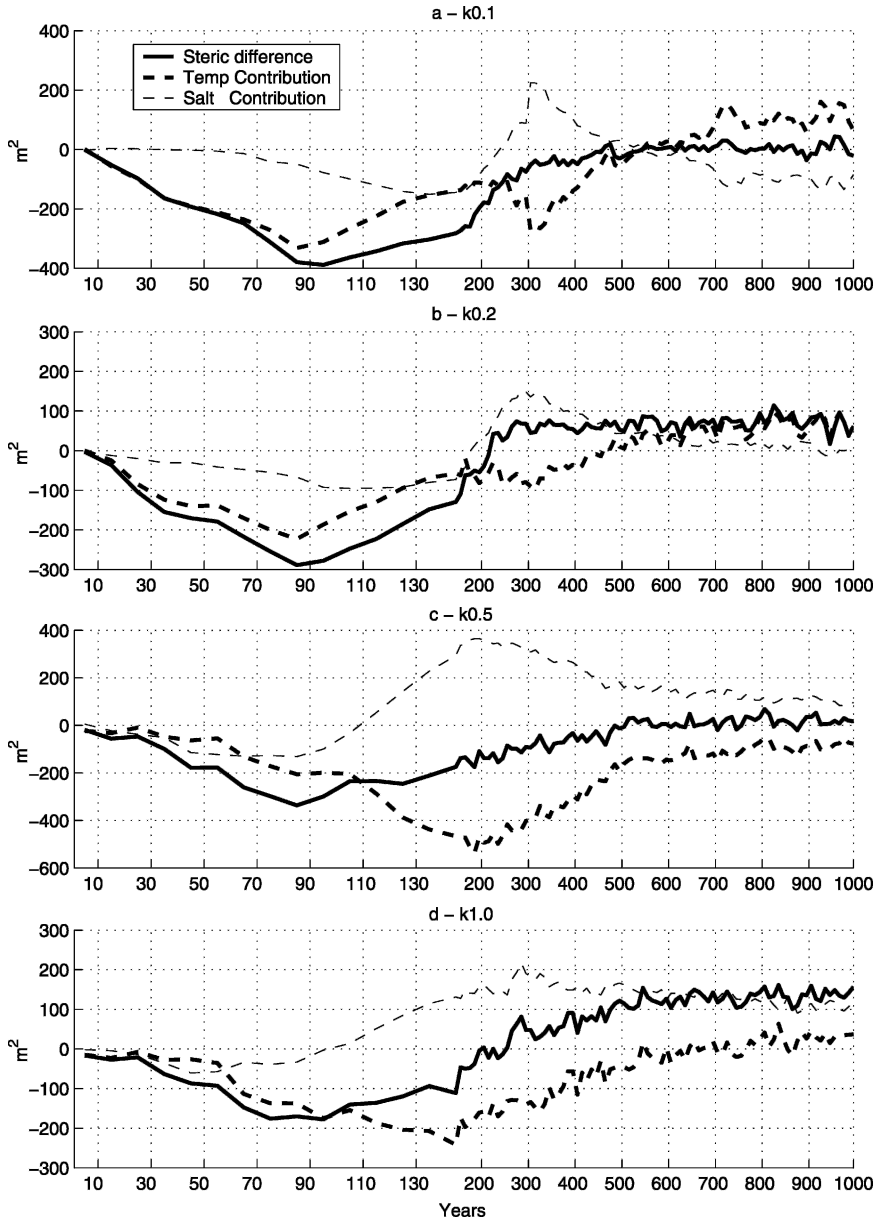

FIG. 3. Steric height gradient anomaly (solid) and its temperature (thick dashed) and salinity (thin dashed) contribution in the Atlantic Ocean for different values of the diapycnal diffusivity: (a) 0.1, (b) 0.2, (c) 0.5, and (d) 1.0 $cm^2\ s^{-1}$. Note the stretching of the horizontal axis.

other case the dominance of the salt component extends shortly over 70 yr of integration.

A direct consequence of our observations is that models with large equilibrium THC overturning may be more sensitive to changes in the salt content in the North Atlantic, as a consequence of enhanced CO_2 in the atmosphere. Hence, even for models showing the same surface heat and freshwater flux perturbations under global warming experiments, the sensitivities to the surface forcing may be different.

4. Vertical heat imbalance

The ocean heat uptake is an important factor in controlling the behavior of the THC under global warming experiments because it affects the temperature, and therefore the density, structure of the ocean. Hence, investigating the relationship between ocean heat uptake and diapycnal diffusivity may give some insight on the behavior of the THC under global warming experiments. In the previous section we have seen how the

competition between temperature and salinity, in determining the steric height gradient, is affected by the diapycnal diffusivity. Here, we investigate which processes are responsible for the temperature change in the deep ocean as the CO_2 increases in the atmosphere, and what is their relation with respect to the diapycnal diffusivity. Addressing these questions can help us understand whether differences in diapycnal diffusivity is one reason for the disagreement among IPCC models in the matter of surface air temperature and sea level rise. We are interested in the different contributions of advection and diffusion to the global ocean vertical heat flux. Local contributions of the vertical heat flux components are presented in order to show how the contribution to the global balance varies from a region to another. We do not include the meridional heat flux components as they do not affect the global heat balance and their discussion goes beyond the purpose of this study. We note however that the storage in the individual regions is small compared to the individual flux convergences, and thus the total meridional flux convergences almost cancel the total vertical flux convergences in the individual regions.

a. Global warming experiment

In our global warming experiments the global ocean warms above 2500 m and cools below this level (Fig. 4a). Cooling at depth occurs in the Northern Ocean (Fig. 4b) and it is due to the reduction of the THC, with consequent reduction of downward advective heat transport in the North Atlantic. The reduction of upwelling in the Tropics (Fig. 4c) compensates for the reduction of heating so that changes in the advective heat flux for the global ocean are small (Fig. 4a).

Heating in the upper 2500 m is due to a decrease in both upward isopycnal diffusion and GM advection and it is concentrated at high latitudes (Figs. 4b,d), in agreement with the adjoint sensitivity study of Huang et al. (2003b, their Fig. 5). Surface heating in global warming experiments leads to less steep isopycnal slopes, which explain the decrease in GM flux. Moreover, with increasing temperature, the density field becomes more dependent on the temperature field, because of the nonlinear dependence of the expansion coefficients on temperature and salinity. Hence, the angle between isopycnals and isotherms decreases, leading to a decrease of isopycnal temperature gradient and lastly of the isopycnal flux, as noted by Gregory (2000).

Surface warming leads to greater vertical temperature gradient and increased diapycnal diffusion in the tropical region (Fig. 4c). On the other hand, in dynamically active regions like the Northern and Southern Ocean the downward diapycnal flux decreases compensating the decrease of the upward isopycnal flux (Figs. 4b,d). As pointed out in Dalan et al. (2005, their Fig. 10), the heat balance at the high latitudes has isopycnal diffusion and diapycnal diffusion acting in the same locations. Isopycnal diffusion removes heat from the deep ocean, thus tending to increase the vertical temperature gradient, while diapycnal diffusion tends to relax this gradient by pumping heat downward. A similar tendency to compensate occurs in global warming experiments: reduction of isopycnal fluxes leads to warming at depth and a relatively small vertical temperature gradient, which then leads to a decrease in the downward diapycnal diffusion.

In Fig. 5, the heat flux anomalies for the Northern Ocean and the Tropics are separated for the Atlantic and Pacific basins. It is clear that the Northern Ocean anomalous fluxes are representative of the North Atlantic (Figs. 5a,b). The area-integrated diapycnal flux anomaly in the tropical Pacific is about 3 times as large as in the tropical Atlantic because the area coverage of the Pacific is twice the Atlantic's; however, the decreased upwelling in the Tropics is greater in the tropical Atlantic than in the tropical Pacific (Figs. 5c,d).

The analysis of vertical heat fluxes in a global warming experiment is also presented by Gregory (2000). At 160-m depth the anomalous fluxes consist of: reduction of convection in the Northern Ocean, reduction of upwelling in the tropical region and reduction of upward isopycnal diffusion in the Southern Ocean. The total heat flux anomaly in the Southern Ocean and Tropics are respectively 0.55 and 0.59 Wm^{-2}, more that three times the anomaly in the Northern Ocean (0.16 Wm^{-2}).

Qualitatively our results agree with Gregory (2000) in the Tropics and in the Northern Ocean, allowing for the fact that in this model the role of convection is replaced by GM advection and isopycnal diffusion (Dalan et al. 2005). In the Southern Ocean we find that reduction of both isopycnal diffusion and GM advection are the major contributors to the increased heat flux. Quantitatively, we note that the vertical heat balance sensibly depends on depth (Fig. 4). At high latitudes, the global heat flux anomaly decreases with depth from a value of 0.5 Wm^{-2} at the surface (Figs. 4b,d). At the Tropics the anomaly is roughly constant at 0.2 Wm^{-2} between the surface and 2000 m, then decreasing with depth until the bottom of the ocean (Fig. 4c). Therefore, above 400 m both Northern and Southern Oceans contribute the most to the global heat flux anomaly, while below this level the Tropics present the highest anomaly.

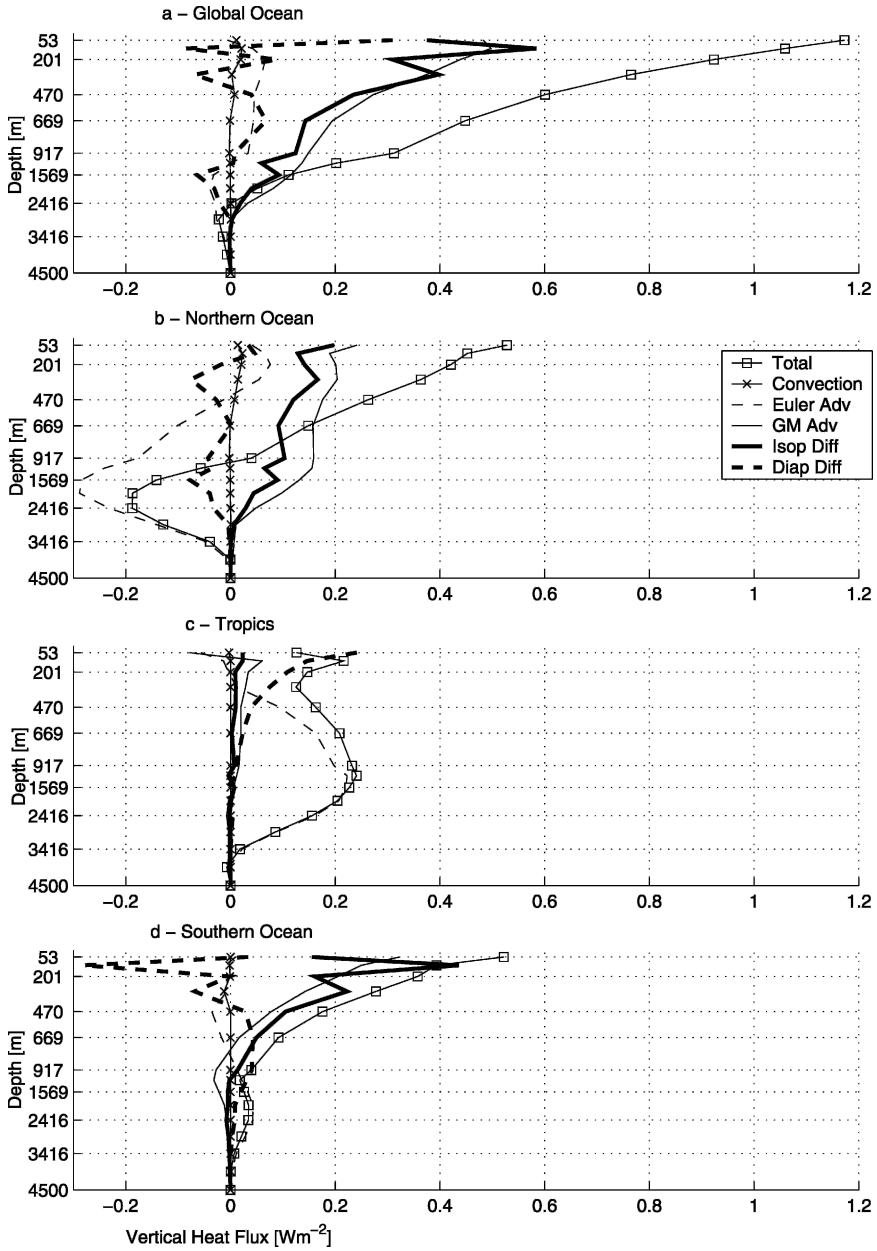

FIG. 4. Global warming experiment. Vertical heat flux anomalies for (a) global ocean, (b) Northern Ocean, (c) Tropics, and (d) Southern Ocean for diapycnal diffusivity 0.5 cm^2 s^{-1}, averaged from years 66–75 of simulation. Positive (negative) sign indicates increase (decrease) for downward fluxes or decrease (increase) for upward fluxes with respect to equilibrium. Upward fluxes are isopycnal diffusion, GM advection, and convection. Downward fluxes are advection and diapycnal diffusion.

b. Sensitivity to diapycnal diffusion

Because the anomalous isopycnal and GM fluxes are the main contributors to the total anomalous heat flux (Fig. 4a), it is natural to think that, by changing isopycnal and/or thickness diffusivities, the amount of heat penetrating the ocean would change accordingly. This is not the case as Huang et al. (2003c) found. Employing the same configuration of the MIT EMIC used in this study,[2] the authors changed both isopycnal and thickness diffusivities by a factor of 2. The anomalous

[2] The MIT Ocean Model code was used instead of MOM2.

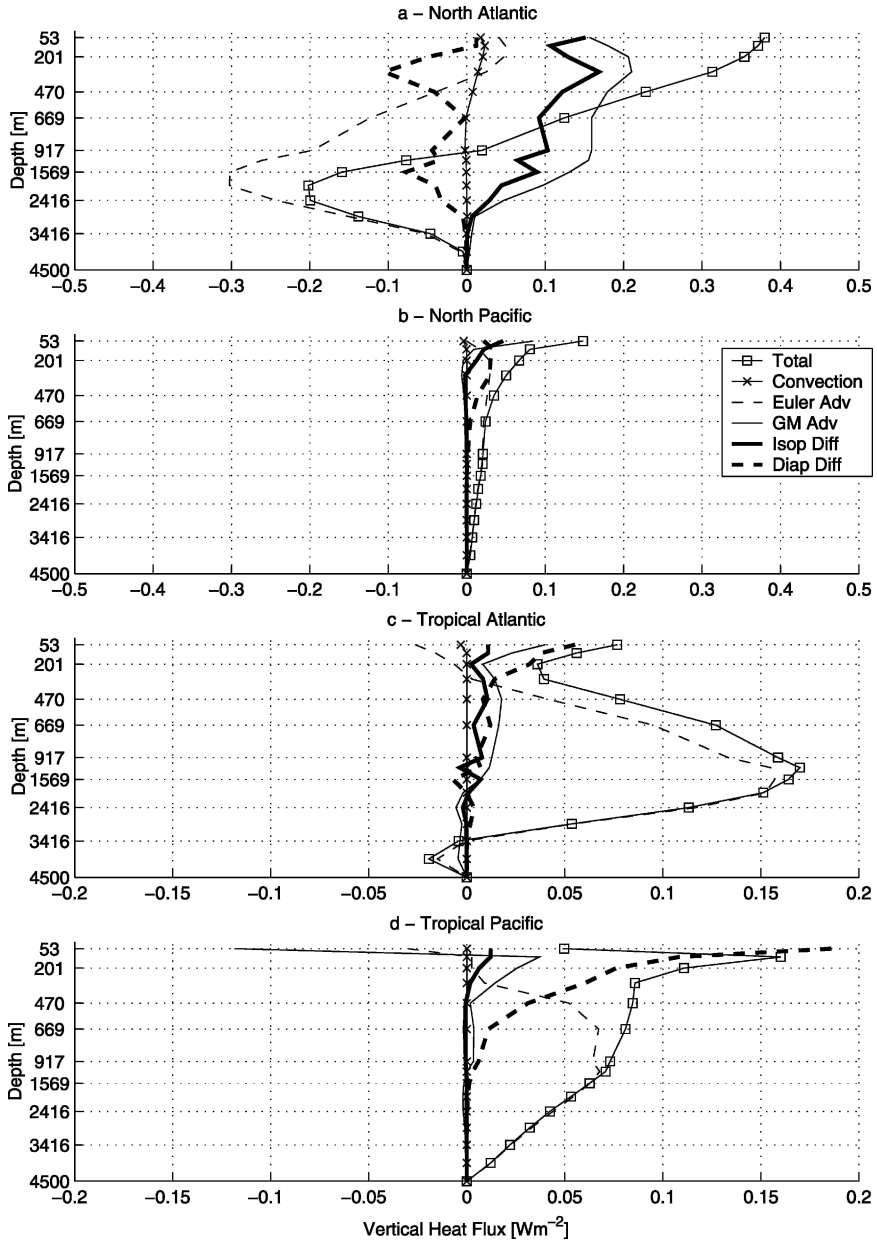

FIG. 5. Global warming experiment, as in Fig. 4, but for vertical heat flux anomalies of the (a) North Atlantic, (b) North Pacific, (c) tropical Atlantic, and (d) tropical Pacific for diapycnal diffusivity 0.5 cm^2 s^{-1}, averaged from years 66–75 of simulation.

heat flux from isopycnal diffusion and GM advection varied, although only slightly, in the same direction as the parametric change (their Fig. 11), and the total anomalous heat flux did not vary appreciably. The same does not happen when the diapycnal diffusion changes, since the total anomalous heat flux entering the ocean sensibly increases at all depths as the diapycnal diffusion increases (Fig. 6).

In global warming simulations the anomalous fluxes behave in the same way for all simulations given varying diapycnal diffusivity (Fig. 6). The major contributions to the heat uptake by the ocean are due to the reduction of isopycnal and GM fluxes at all depths. The magnitude of the total anomaly is directly proportional to the diffusivity, implying a greater heat penetration for high diapycnal diffusivity (Fig. 6). The reason for the increase is not directly related to the increase of diffusive heat from the ocean surface, as common physical intuition might suggest. Maximum warming is localized at high latitudes of the Atlantic Basin and in

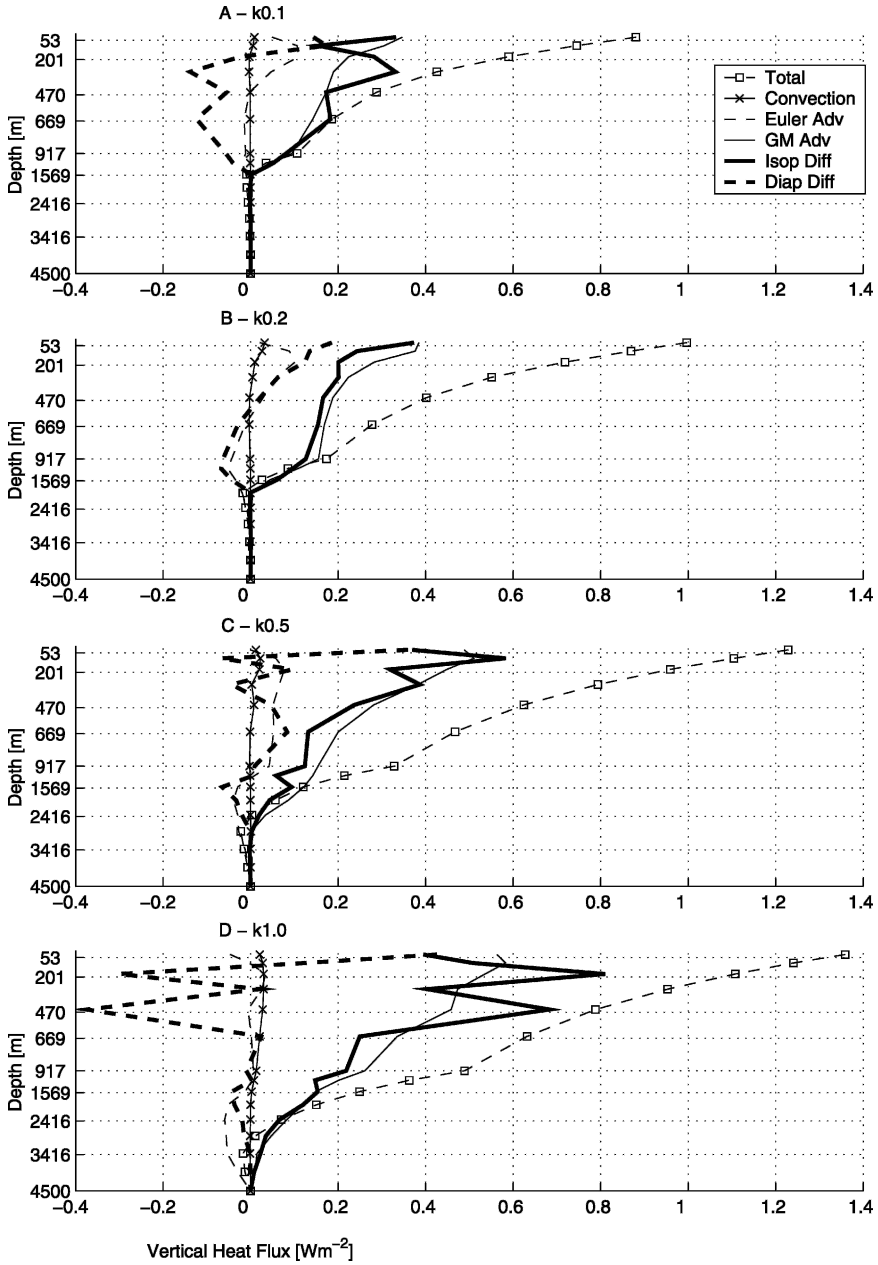

FIG. 6. Changes in vertical heat fluxes due to global warming for the global ocean and for diapycnal diffusivity (a) 0.1, (b) 0.2, (c) 0.5, and (d) 1.0 cm^2 s^{-1}, averaged from years 66–75 of simulation. Positive (negative) sign indicates increase (decrease) for downward fluxes or decrease (increase) for upward fluxes with respect to equilibrium. Upward fluxes are isopycnal diffusion, GM advection, and convection. Downward fluxes are advection and diapycnal diffusion.

the Southern Ocean (Fig. 7), where isopycnal diffusion and GM advection dominate, both in magnitude in the control runs (Dalan et al. 2005) and in tendency in global warming experiments (Fig. 6). Note that the relative small warming at 50°N in the Atlantic basin (Fig. 7) is caused by a southward shift of the Gulf Stream, as a consequence of the slowdown of the Thermohaline Circulation.

The connection between elevated diapycnal diffusivity and ocean heat uptake, given by isopycnal diffusion and GM advection, is found in the temperature structure of the ocean in the control run. The thickness of

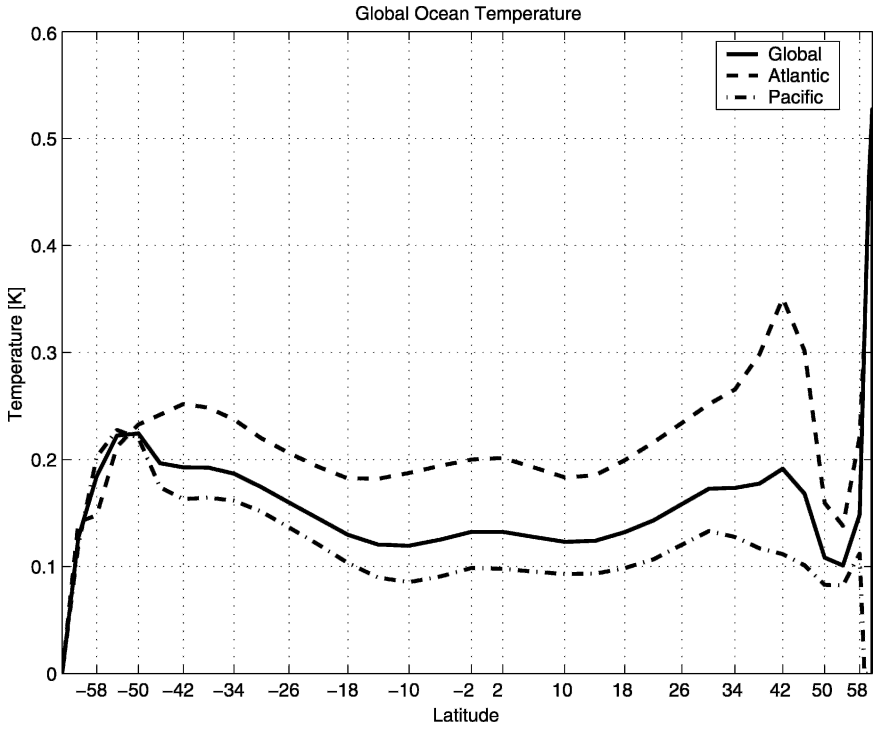

FIG. 7. Meridional distribution of global ocean temperature anomaly at the time of CO_2 doubling for diapycnal diffusivity 0.5 $cm^2\ s^{-1}$.

the thermocline is proportional to the diapycnal diffusivity, due to the larger heat diffusion from the surface of the ocean. Hence, at high latitudes the isopycnal slope increases as the thermocline deepens, followed by an increase of isopycnal and GM fluxes.[3] In global warming simulations, the surface warming reduces the isopycnal slopes in high latitudes of the North Atlantic (Fig. 8) leading to a decrease of upward GM and isopycnal fluxes. The magnitude of the decrease is proportional to their control values, hence to the thickness of the thermocline and lastly to the diapycnal diffusivity. We recall that in this version of the MIT EMIC, the role of convection is inhibited by the efficient mixing caused by isopycnal diffusion and GM advection. If the maximum isopycnal slope is reduced, convection plays a significant role in the vertical heat balance at equilibrium (Dalan et al. 2005, their Fig. A2) and possibly also under global warming experiments.

c. Comparison with CMIP2

In simulations with a 1% yr^{-1} increase in CO_2 concentration, performed as part of the coupled model intercomparison project (see online at http://www-pcmdi.llnl.gov/cmip.cmiphome.html), the increase in global mean SAT at the time of CO_2 doubling ranged from 1.32 to 2.15°C (Covey et al. 2000) for different models. Similarly the results for SLR due to thermal expansion of the ocean ranged from 6.5 to 14.5 cm (S. Raper 2000, personal communication). The different model responses are associated with differences in the models' effective climate sensitivity and rate of heat uptake. Sokolov et al. (2003) showed that changes in the global mean SAT and SLR simulated by different AOGCMs can be reproduced by the MIT 2D climate model (Sokolov and Stone, 1998) with an appropriate choice of the 2D model's climate sensitivity and its rate of heat uptake in the ocean. The latter is simulated by diffusing heat anomalies into the deep ocean with an effective global mean diffusion coefficient, K_v, which represents the net effect of all oceanic processes: advection, diffusion and convection.

Sensitivity experiments showed little dependence of the total heat uptake by the ocean on the isopycnal diffusivity and GM parameter when the latter are varied together (Huang et al. 2003c). Moreover, to the lowest order, advection by the THC is directly proportional to the diapycnal diffusivity. Hence, we can expect a strong relationship between K_v and the diapycnal dif-

[3] At equilibrium all fluxes increase for increasing diapycnal diffusion (Dalan et al. 2005, their Fig. 11).

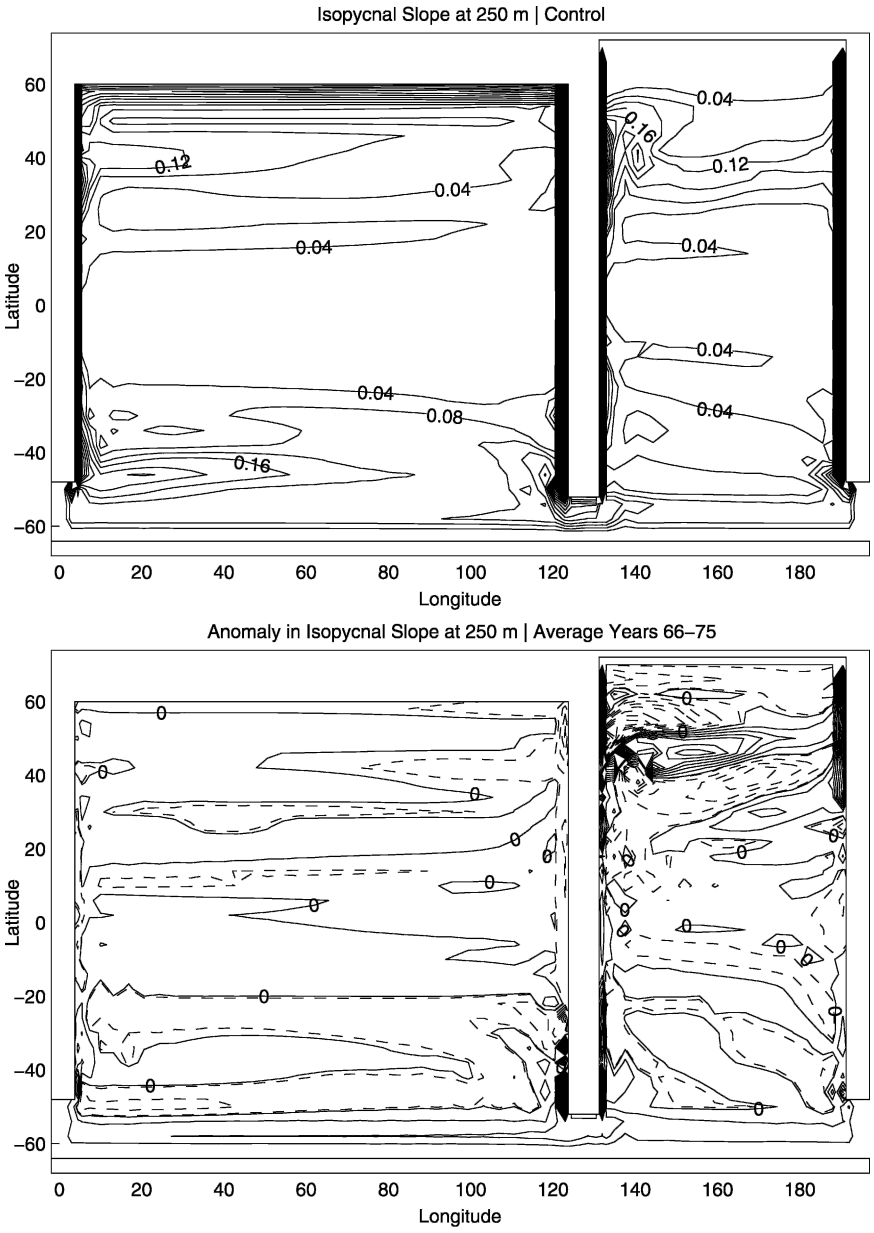

FIG. 8. Modulus of the (top) isopycnal slope and (bottom) its anomaly due to global warming at 250-m depth for diapycnal diffusivity 0.5 $cm^2\ s^{-1}$. Solid line denotes positive values and dashed line denotes negative values.

fusivity. Indeed in our GCM we can vary the ocean heat uptake by varying the diapycnal diffusivity (Fig. 6).

This diapycnal mixing parameter mimics the effect of processes such as the wind stirring at the surface of the ocean and the internal waves, mostly induced by the breaking of tidal waves over the bottom topography. Numerical models make use of different parameterization schemes to account for the spatial variations of the diapycnal mixing, while, for the sake of simplicity and to aid our understanding of the experimental results, we chose a uniform diapycnal diffusivity. Quantity such as SAT and SLR depend on the effective diffusivity K_v, and our results help us to understand the differences among CMIP2 models.

Table 1 shows how varying the diapycnal mixing coefficient from 0.1 to 1.0 $cm^2\ s^{-1}$ changes the response of our model. The different responses of the model give an estimate of the uncertainty in global warming projections due to uncertainty in the diapycnal diffusion. Table 1 also gives the values of K_v in the 2D model that

TABLE 1. Model results at year 70 in the global warming scenario. (b) Surface air temperature anomaly, (c) sea level rise due to thermal expansion at the time of doubling CO_2, and (d) effective diffusivity of the MIT 2D climate model in global warming experiments with (a) different diapycnal diffusivity.

a	Diapycnal diffusivity ($cm^2\ s^{-1}$)	0.1	0.2	0.5	1.0
b	Change in SAT (K)	1.83	1.68	1.57	1.46
c	SLR (cm)	9.2	10.3	12.1	13.1
d	Equivalent K_v ($cm^2\ s^{-1}$)	5.0	7.5	37	125

allow it to mimic the response of our model for different values of the diapycnal diffusivity. These values of K_v cover most of the range of the CMIP2 models, which goes from 4 to 50 $cm^2\ s^{-1}$ (Sokolov et al. 2003, their Fig. 1). Thus the MIT-EMIC with varying values of the diapycnal diffusivity can also be used in sensitivity studies where the effect of different rates of oceanic heat uptake need to be taken into account (Webster et al. 2003). We note that the range of values for the change in SAT and SLR shown in table 1 are not as large as for the CMIP2 models, because the MIT EMIC results shown in Table 1 are for a fixed climate sensitivity of 2.8 K, whereas the climate sensitivity of the CMIP2 models ranges from 1.9 to 4.2 K.

5. Conclusions

We analyzed the sensitivity of the climate to diapycnal diffusivity for a global warming scenario focusing on the behavior of the THC and on the rate of heat uptake by the ocean. This study is the first to explore the sensitivity to diapycnal diffusion of the ocean using a coupled model with a 3D ocean component.

Increasing the carbon dioxide level in the atmosphere at a rate of 1% yr^{-1} for 75 yr leads to a slowdown of the THC circulation for about 100 yr and recovery afterward. The rate at which the circulation recovers and the percentage recovery at the end of the simulation vary with the diapycnal diffusion in an unpredictable fashion. For the largest (1.0 $cm^2\ s^{-1}$) and smallest (0.1 $cm^2\ s^{-1}$) values of the diapycnal diffusivity, recovery is slow and incomplete at the end of the 1000 yr integration. For diapycnal diffusivity equal to 0.5 $cm^2\ s^{-1}$ the circulation recovers rapidly, while for diapycnal diffusivity equal to 0.2 $cm^2\ s^{-1}$ the circulation first recovers completely its control strength. For the first 60–70 yr of integration, what differentiates the response of the climate system (as the diapycnal diffusion varies) is the relative contribution of temperature and salinity in determining the evolution of steric height gradient between North and South Atlantic. In climate systems with small diapycnal diffusivity, the temperature variations largely explain the changes in steric height gradient, while in highly diffusive ocean models, the salinity variations are comparable to the temperature's in terms of steric height. Thus, the sensitivity of the model to surface heat and moisture flux depends on the diapycnal diffusivity to the extent that the latter parameter controls the strength of the advective and diffusive processes at equilibrium, and by consequence the strength of their rate of change. Both the strength of the THC and the thickness of the thermocline highly depend on the diapycnal diffusivity. As a consequences also the advective timescale and the magnitude of the GM advective fluxes and both isopycnal and diapycnal fluxes are related to the diapycnal diffusivity. Therefore the relation between sensitivity to surface forcing and diapycnal diffusivity is likely to be an indirect consequence of the relation between the latter parameter and the state of the climate at equilibrium.

The rate of ocean heat uptake under global warming experiments increases with diapycnal diffusivity. The increase in ocean heat content is related to the decrease in bolus velocity (GM) advection and isopycnal diffusion that are the major heat sinks. The role of convection is negligible in this version of the model since first GM advection and then isopycnal diffusion, efficiently mix the surface ocean. At high latitudes, the rise in sea surface temperature due to global warming leads to a decrease of isopycnal slope and in the temperature gradient along isopycnals. Consequently both GM advection and isopycnal diffusion are reduced inducing warming of the subsurface ocean. At equilibrium, the magnitude of these processes is greater for a thicker thermocline, thus for larger diapycnal diffusivity. In global warming experiments the decrease in upward isopycnal diffusion and GM advection is proportional to their value at equilibrium; hence, the rate of ocean heat uptake is larger for larger diapycnal diffusivity.

The uncertainty in the global value of the diapycnal diffusivity reflects on the uncertainty in ocean heat uptake under global warming scenarios, which in turn regulates the increase in surface air temperature (SAT) and sea level rise (SLR). Our calculations suggest that an increase of the diapycnal diffusivity by a factor 10 (from 0.1 to 1.0 $cm^2\ s^{-1}$) leads, at the time of doubling CO_2, to a decrease of SAT of 0.4 K and an increase of SLR due to thermal expansion of 4 cm.

Acknowledgments. We thank the two anonymous reviewers for useful comments and suggestions that improved the clarity of the manuscript. This research was supported in part by MIT's Joint Program on the Science and Policy of Global Change and in part by the Office of Science (BER), U.S. Department of Energy, Grant DE-FG02-93ER61677.

REFERENCES

Bryan, F., 1987: Parameter sensitivity of primitive equation ocean general circulation models. *J. Phys. Oceanogr.,* **17,** 970–985.

Bryan, K., 1984: Accelerating the convergence to equilibrium of ocean–climate models. *J. Phys. Oceanogr.,* **14,** 666–673.

Covey, C., K. M. Achuta Rao, S. J. Lambert, and K. E. Taylor, 2000: Intercomparison of present and future climates simulated by coupled ocean-atmosphere GCMs. PCMDI Rep. 66, 52 pp.

Dalan, F., P. H. Stone, I. V. Kamenkovich, and J. R. Scott, 2005: Sensitivity of the ocean's climate to diapycnal diffusivity in an EMIC. Part I: Equilibrium state. *J. Climate,* **18,** 2460–2481.

Forest, C. E., P. H. Stone, A. P. Sokolov, M. R. Allen, and M. D. Webster, 2002: Quantifying uncertainties in climate system properties with the use of recent climate observations. *Science,* **295,** 113–117.

Ganopolsky, A., V. Petoukhov, S. Rahmstorf, V. Brovkin, M. Claussen, A. Eliseev, and C. Kubatzki, 2001: CLIMBER-2: A climate system model of intermediate complexity. Part II: Model sensitivity. *Climate Dyn.,* **17,** 735–751.

Gent, P. R., and J. C. McWillams, 1990: Isopycnal mixing in ocean circulation models. *J. Phys. Oceanogr.,* **20,** 150–155.

Gregory, J. M., 2000: Vertical heat transports in the ocean and their effect on time-dependent climate change. *Climate Dyn.,* **16,** 501–515.

Hansen, J., G. Russel, D. Rind, P. Stone, A. Lacis, S. Lebedeff, R. Ruedy, and L. Travis, 1983: Efficient three-dimensional global models for climate studies: Model I and II. *Mon. Wea. Rev.,* **111,** 609–662.

Houghton, J. T., Y. Ding, D. J. Griggs, M. Noguer, P. J. van der Linden, X. Dai, K. Maskell, and C. A. Johnson, 2001: *Climate Change 2001: The Scientific Basis*. Cambridge University Press, 881 pp.

Huang, B., P. H. Stone, and C. Hill, 2003a: Sensitivities of deep-ocean heat uptake and heat content to surface fluxes and subgrid-scale parameters in an ocean general circulation model with idealized geometry. *J. Geophys. Res.,* **108,** 3015, doi:10.1029/2001JC001218.

——, ——, A. P. Sokolov, and I. V. Kamenkovich, 2003b: The deep-ocean heat uptake in transient climate change. *J. Climate,* **16,** 1352–1363.

——, ——, ——, and ——, 2003c: Ocean heat uptake in transient climate change: Mechanisms and uncertainty due to subgrid-scale eddy mixing. *J. Climate,* **16,** 3344–3356.

Huang, R. X., 1999: Mixing and energetics of the oceanic thermohaline circulation. *J. Phys. Oceanogr.,* **29,** 727–746.

Hughes, T. C. M., and A. J. Weaver, 1994: Multiple equilibria of an asymmetric two-basin ocean model. *J. Phys. Oceanogr.,* **24,** 619–637.

Jiang, S., P. H. Stone, and P. Malanotte-Rizzoli, 1999: An assessment of the Geophysical Fluid Dynamics Laboratory ocean model with coarse resolution: Annual-mean climatology. *J. Geophys. Res.,* **104,** 25 623–25 645.

Kamenkovich, I. V., A. P. Sokolov, and P. H. Stone, 2002: An efficient climate model with a 3D ocean and a statistical-dynamical atmosphere. *Climate Dyn.,* **19,** 585–598.

——, ——, and ——, 2003: Feedbacks affecting the response of the thermohaline circulation to increasing CO_2: A study with a model of intermediate complexity. *Climate Dyn.,* **21,** 119–130.

Knutti, R., and T. F. Stocker, 2002: Limited predictability of the future thermohaline circulation close to an instability threshold. *J. Climate,* **15,** 179–186.

Ledwell, J. R., E. T. Montgomery, K. L. Polzin, L. C. St. Laurent, R. W. Schmitt, and J. M. Toole, 2000: Evidence for enhanced mixing over rough topography in the abyssal ocean. *Nature,* **403,** 179–182.

Manabe, S., and R. J. Stouffer, 1999: Are two modes of thermohaline circulation stable? *Tellus,* **51A,** 400–411.

Marotzke, J., 1997: Boundary mixing and the dynamics of three-dimensional thermohaline circulation. *J. Phys. Oceanogr.,* **27,** 1713–1728.

Munk, W., and C. Wunsch, 1998: Abyssal recipes II: Energetics of tidal and wind mixing. *Deep-Sea Res.,* **45,** 1977–2010.

Pacanowski, R. C., 1996: MOM2 version 2.0: Documentation user's guide and reference manual. Geophysical Fluid Dynamics Laboratory Tech. Rep. 3.2, 232 pp.

Park, Y. G., and K. Bryan, 2000: Comparison of thermally driven circulations from a depth-coordinate model and an isopycnal-layer model. Part I: Scaling-law sensitivity to vertical diffusivity. *J. Phys. Oceanogr.,* **30,** 590–605.

Polzin, K. L., J. M. Toole, J. R. Ledwell, and R. W. Schmitt, 1997: Spatial variability of turbulent mixing in the abyssal ocean. *Science,* **276,** 93–96.

Prinn, R., and Coauthors, 1999: Integrated global system model for climate policy assessment: Feedbacks and sensitivity studies. *Climatic Change,* **41,** 469–546.

Redi, M. H., 1982: Oceanic isopycnal mixing by coordinate rotation. *J. Phys. Oceanogr.,* **12,** 1154–1158.

Sokolov, A. P., and P. H. Stone, 1998: A flexible climate model for use in integrated assessments. *Climate Dyn.,* **14,** 291–303.

——, C. E. Forest, and P. H. Stone, 2003: Comparing oceanic heat uptake in AOGCM transient climate change experiments. *J. Climate,* **16,** 1573–1582.

Stocker, T. F., and A. Schmittner, 1997: Influence of CO_2 emissions rates on the stability of the thermohaline circulation. *Nature,* **388,** 862–865.

Stone, P. H., and M.-S. Yao, 1990: Development of a two-dimensional zonally averaged statistical–dynamical model. Part III: The parameterization of the eddy fluxes of heat and moisture. *J. Climate,* **3,** 726–740.

Thorpe, R. B., J. M. Gregory, T. C. Johns, R. A. Woods, and J. F. B. Mitchell, 2001: Mechanisms determining the Atlantic thermohaline circulation response to greenhouse gas forcing in a non-flux-adjusted coupled climate model. *J. Climate,* **14,** 3102–3116.

Webster, M., and Coauthors, 2003: Uncertainty analysis of climate change and policy response. *Climate Change,* **61,** 295–320.

Zhang, J., R. W. Schmitt, and R. X. Huang, 1999: The relative influence of diapycnal mixing and hydrologic forcing on the stability of the thermohaline circulation. *J. Phys. Oceanogr.,* **29,** 1096–1108.